Carbohydrate Polymers 88 (2012) 1304–1312

Contents lists available at SciVerse ScienceDirect

Carbohydrate Polymers

journal homepage: www.elsevier.com/locate/carbpol

Electrospun anti-adhesion barrier made of chitosan alginate for reducing peritoneal adhesions

Jung-Jhih Chang[a], Yen-Hsien Lee[b], Meng-Hsiu Wu[a], Ming-Chien Yang[a,*], Chiang-Ting Chien[c,**]

[a] Department of Materials Science and Engineering, National Taiwan University of Science and Technology, Taipei 106, Taiwan, ROC
[b] Graduate Institute of Applied Science and Technology, National Taiwan University of Science and Technology, Taipei 106, Taiwan, ROC
[c] Department of Medical Research, National Taiwan University Hospital and National Taiwan University College of Medicine, Taipei 100, Taiwan, ROC

ARTICLE INFO

Article history:
Received 19 December 2011
Received in revised form 4 February 2012
Accepted 5 February 2012
Available online 14 February 2012

Keywords:
Electrospun mats
Anti-adhesion
Chitosan
Sodium alginate
Animal model

ABSTRACT

In this study, novel anti-adhesion mat made of chitosan alginate was fabricated via electrospinning. The structure and morphology of electrospun membrane were examined using a field-emission scanning electron microscope and confocal laser scanning microscope. The degree of disintegration of the electrospun mat was assessed. The results showed that the degree of disintegration in DMEM for chitosan alginate mat was 64% of that of conventional calcium alginate mat after 5 days. In addition, the tissue anti-adhesion potential was evaluated with in vitro cell adhesion model and in vivo rat model. About 40% of the animals treated with chitosan alginate exhibited no tissue adhesion between injured peritoneum and cecum. The result demonstrated that chitosan alginate was effective in reducing the formation of tissue adhesion.

1. Introduction

In order to prevent postoperative adhesions, various pharmacological and barrier approaches to treat adhesion have been developed. Recently, the potential therapeutic agents has increased considerably, including steroidal, and non-steroidal anti-inflammatory compounds, tissue plasminogen activator (tPA), and the agents that interfere with specific cytokines or vascular permeability (Cashman, Kennah, Shuto, Winternitz, & Springate, 2010; Yeo & Kohane, 2008). One common approach to prevent adhesion is to place a physical barrier between injured site and the adjacent tissues. Various materials, made of animal tissues, biological materials and synthetic polymers, have been reported to be effective in reducing adhesion both in animal models and in clinical practices.

Seprafilm™ (Genzyme, Cambridge, MA) is a hydrophilic membrane composed of sodium hyaluronate and carboxymethylcellulose. This barrier has shown clinical efficacy to reduce adhesions during the post-operative healing phase (Chuang et al., 2008). However, many surgeons reported that Seprafilm is breakable and sticky (Ward & Panitch, 2011). In addition, hyaluronate degrades quickly and disappears from the injured site soon after application (Way, Hsieh, Chang, Hung, & Chiu, 2010). Furthermore, Seprafilm would increase adhesion in the presence of bacterial peritonitis in a murine model (Kayaoglu, Ozkan, Hazinedaroglu, Ersoy, & Koseoglu, 2005). Interceed™ (Gynecare, Somerville, NJ) is a fabric composed of oxidized regenerated cellulose (ORC) that can significantly reduce adhesions effectively in some animal models and clinical studies. Interceed does seem to provoke a large leukocyte response and can cause mesothelial cell sloughing in mice. However, blood infiltration makes the product ineffective in preventing adhesions, thus surgeons must ensure that all blood is cleared from the surgical field prior to using Interceed™ (Kayaoglu et al., 2005).

To improve the shortcomings of the aforementioned commercial products, anti-adhesion barrier must be more efficient in preventing the occurrence of adhesion. Therefore, many researchers attempt to design novel biomaterials with less complications and higher efficiencies (Bölgen, Vargel, Korkusuz, Menceloğlu, & Pişkin, 2007). In the literature, in vivo studies in animals have demonstrated that N,O-carboxymethylchitosan (NOCC) is safe and efficacious as an anti-adhesion barrier (Diamond et al., 2003). A modified chitosan–dextran gel was used to prevent peritoneal adhesions in a rat model, and significantly reduced the formation of intra-abdominal adhesions without adversely affecting wound healing (Lauder, Garcea, Strickland, & Maddern, 2011). Although chitosan/alginate mixtures have been patented for post-surgical adhesion barrier (Yeo et al., 2006), no product of this material was commercialized up to date.

* Corresponding author. Tel.: +886 2 2737 6528; fax: +886 2 2737 6544.
** Corresponding author. Tel.: +886 2 2312 3456x65720; fax: +886 2 2394 7927.
E-mail addresses: myang@mail.ntust.edu.tw (M.-C. Yang), ctchien@ntuh.gov.tw (C.-T. Chien).

0144-8617/$ – see front matter © 2012 Elsevier Ltd. All rights reserved.
doi:10.1016/j.carbpol.2012.02.011

Chitosan and alginate have been proposed for many biomedical applications for their excellent biocompatibility. Chitosan is a natural-based aminopolysaccharide with a wide variety of useful biological properties, including excellent biocompatibility, biodegradability, hemostatic activity, nontoxicity, antimicrobial activity, and free radical scavenging activities (Anraku et al., 2011; Pillai, Paul, & Sharma, 2009). Hence, chitosan has been investigated for using in a wide variety of biomedical applications, including drug delivery system, and tissue engineering (Bhattarai, Gunn, & Zhang, 2010; Li, Ramay, Hauch, Xiao, & Zhang, 2005; Muzzarelli, 2009, 2010). Alginate is a naturally anionic polysaccharide consisting of 1,4-linked β-D-mannuronic acid (M) and α-L-guluronic acid (G) units. Alginate can form hydrogels, beads, porous sponges, and microfibers. Alginate exhibits excellent biocompatibility, nontoxicity, non-immunogenicity, and biodegradability (George & Abraham, 2006). Furthermore, chitosan and alginate can inhibit lipid peroxidation of phosphatidylcholine and linoleate liposomes (Tomida et al., 2010).

Electrospinning (ES) is a valuable and versatile fabrication method for creating micrometer or nanometer-sized fiber from various types of naturally and synthetic materials for biomedical or tissue engineering applications (Agarwal, Wendorff, & Greiner, 2008; Lee, Jeong, Kang, Lee, & Park, 2009; Muzzarelli, 2011). In the electrospinning process, fiber mats were formed by applying a high voltage to polymer solutions flowing through a syringe. The fibrous mats were collected on a grounded substrate (Rutledge & Fridrikh, 2007). Electrospun fibrous mats possess high surface areas, high porosities, and variable fiber diameters (Agarwal, Wendorff, & Greiner, 2009). Currently anti-adhesion barrier made of electrospun mat was little studied. Only poly(lactide-co-glycolide) (Zong et al., 2004), poly(ε-caprolactone) (Bölgen et al., 2007), and polylactide-poly(ethylene glycol) triblock copolymer (PELA) (Yang, Chen, Xiong, Xiong, & Wang, 2009) have been reported. Both polymers are synthetic and non-bioactive.

Many methods have been employed to reduce the formation of adhesions. However, no single approach has been wholly satisfactory, because the anti-adhesion barrier often imposes several limitations of their final properties. Chitosan film can be too brittle to handle and will degrade very slowly (Paulo et al., 2009). Chitosan gel is still defective because it is highly flowable (Zhang, Xu, & Zhou, 2006). In our recent studies, we have first fabricated chitosan alginate fibrous mat with core-sheath structure via electrospinning (Chang, Lee, Wu, Yang, & Chien, 2012). Such a mat exhibited higher flexibility, hydrophilicity, and degradability than pure chitosan film. The goal of this study is to employ this chitosan alginate mat as a novel anti-adhesion barrier to prevent peritoneal adhesions. In the literature, alginate is not adhesive to cells and serum proteins (Jeong, Krebs, Bonino, Khan, & Alsberg, 2010), and chitosan can reduce the formation of adhesion layer (Zhang et al., 2006). The morphology and structure of fibrous mats were investigated by field-emission scanning electronic microscope (FE-SEM) and confocal laser scanning microscope (CLSM). The anti-adhesion ability and cytocompatibility of the ES mat was assessed. In addition, the in vivo performance of the ES mat for peritoneal operation was evaluated histologically using rat models.

2. Experimental

2.1. Materials

Sodium alginate (Mw 220 kDa) and chitosan (Mw 200 kDa) were purchased from Acros, USA. 1-Ethyl-3-(-3-dimethylaminopropyl) carbodiimide hydrochloride (EDC), fluorescein isothiocynate (FITC), rhodamine B isothiocynate (RITC), glycerol, ethanol, 3-(4,5-dimethyllthiazol-2-yl)-2,5-diphenyl-tetrazolium bromide (MTT), acetic acid, and 3,3′-diaminobenzidine (DAB) were purchased form Sigma, USA. All chemicals were used without any further purification.

2.2. Preparation of polymer solutions

The 1.5 wt% alginate solution was prepared by dissolving sodium alginate powder in 50 wt% glycerol at room temperature for 1 day under stirring to form a homogeneous solution. Chitosan was dissolved in an aqueous solution containing 5 wt% acetic acid at 25 °C under stirring for 1 day to form a homogeneous solution of 1 wt%. Afterwards, the chitosan solution was mixed with equal volume of ethanol as a coagulant solution.

2.3. Electrospinning

The electrospinning system was consisting of a power supply (ES30P, Gamma High Voltage Research, USA), a syringe pump (LSP04-1A, Baoding Longer Precision Pump Co., Ltd., China), and a coagulating bath. The alginate solution was loaded into a 5 ml syringe with a needle spinneret (OD 1.07 mm, ID 0.77 mm). In this study, the flow rate was 0.5 ml/h, the applied voltage was 14 kV, and the distance between the needle and the coagulating bath was 70 mm. The resulting fibers were labeled as chitosan alginate. For comparison, alginate solution was electrospun into 80 wt% ethanol aqueous solution containing 10 wt% $CaCl_2$. The resulting fibers were labeled as calcium alginate. All these resulting fibers were immersed in ethanol for 1 h and then rinsed with ethanol to remove residual glycerol. Afterwards, the samples were dried at 60 °C for 1 d.

2.4. Characterization

The morphology of the ES mats was examined using a field-emission scanning electronic microscope (FE-SEM, JSM-6500F, JEOL, Japan), and a confocal microscope (LSM 510 META, Carl Zeiss Inc., USA). According to our previous work, the structure of the resulting fiber can be observed using fluorescence-labeled polymers (Lee, Chang, Lai, Yang, & Chien, 2011; Lee, Ryu, Je, & Kim, 2011). Briefly, alginate was labeled with FITC (alginate-FITC) and chitosan was labeled with RITC (chitosan-RITC). These labeled polymers were mixed with neat polymers to prepare ES mat as described in previous section. Cryomicrotome sections of the ES mat were then examined using a confocal microscope.

2.5. In vitro disintegration of ES mat

The ES mats disintegrate gradually during in vitro tests. To investigate the disintegration behavior, the mass loss of the ES mat was determined under static conditions. Briefly, the dried samples were immersed in 10 ml of Dulbecco's modified Eagle medium (DMEM) solution at ambient temperature. At a specific time, samples were washed with deionized water three times, and dried at 60 °C to constant weight and the fiber morphology was examined using SEM. The mass loss of each samples were determined according to the following equation:

$$\text{Mass loss}\ \ (\%) = 100\% \times \frac{W_{\text{before}} - W_{\text{after}}}{W_{\text{before}}}$$

where W_{before} and W_{after} are the weights of dry sample before and after swelling, respectively. Each experiment was repeated six times and the average value was recorded.

2.6. In vitro cytocompatibility tests

2.6.1. Electric cell–substrate impedance sensing (ECIS)

Electric cell–substrate impedance sensing (ECIS) is a device developed to monitor the impedance of small gold electrodes used as substrata for cells in culture. ECIS technology is not only capable of producing quantitative data, but is also able to monitor experiments in real-time (Giaever & Keese, 1984). This system has been extensively studied and used to detect subtle changes in the cell–substrata interactions including cell motion. ECIS measures the interaction between cells and the substrate to which they are attached via gold-film electrodes placed on the bottom of culture dishes. Through these electrodes, the ability of the cell monolayer to impede a non-invasive AC signal can be measured. As cultured cells attach and spread onto the electrodes, the current is impeded proportional to the number of attached cells, the number of tight junctions between cells and the shortness in distance between the cells and the substratum (McCoy & Wang, 2005).

In this study, we used the ECIS Model 800 (Applied BioPhysics, Troy, USA) with ECIS electrode array chip (8 W10E+, Applied BioPhysics, Troy, USA) to monitor cell behavior. Each array chip is comprised of eight wells. The surface of each well contains an active gold microelectrode (250 μm in diameter) for detecting the current flow through the medium. The array holder was placed in a standard cell culture incubator (37 °C, in 5% CO_2). The array chips were equilibrated with 200 μl of DMEM in the incubator at cell culture conditions overnight. Then, 1×10^5 L929 cells were seeded to each well containing 200 μl of either DMEM or extract of the sample. During the incubation, cell attachment and spreading were followed by means of impedance (Giaever & Keese, 1984). Data were collected continuously at 15 kHz and the sampling interval was 150 s.

2.6.2. Cell proliferation on ES mat

The ability of L929 cells to proliferate on the ES mat was further evaluated. Briefly, 2 ml of serum free DMEM were added in each well containing a piece of the mat (1 cm × 1 cm). After incubating at 37 °C for 24 h, the medium was replaced with DMEM supplemented with 10% FBS and 1% penicillin/streptomycin. L929 fibroblasts were than seeded on the fibrous mat (1×10^4 cells/well) and incubated for 5 days. The medium was replaced every other day. After culturing for 1, 3 and 5 days, the proliferation on each sample was evaluated by the MTT assay.

2.6.3. Annexin V-FITC and propidium iodide staining apoptosis tests

The L929 fibroblast cells were cultured in 6-well plates (1×10^5 cells/well) and culturing with the samples. The cells were then incubated for 24 h. The subsequent procedures were carried out according to the manufacturer's manual of the Annexin V-FITC kit (Strong Biotech Corporation, Taiwan). Briefly, the cells were washed three times with ice-cold phosphate buffer saline (PBS) and suspended at a concentration of 1×10^4 cells/well followed by the additions of FITC Annexin V and propidium iodide (PI) and left for 15 min in the dark at room temperature. The samples were then analyzed using a flow cytometer (Gallios™ flow cytometer, Beckman Coulter, Inc., USA) within 1 h. Early apoptosis and late apoptosis/necrosis were expressed as the percentages of Annexin V^+/PI^- and Annexin V^+/PI^+ positive cells.

2.7. Animal study

All the animal experiments were conducted with the ethical approval of National Taiwan University Hospital Animal Center. A total of 40 adult female Wistar rats, weighing 220–240 g were used for this work. All rats were housed at a constant temperature and humidity in a room with an artificial 12 h light/dark cycle and allowed free access to food and water.

In this work, the rats were anesthetized with Zoletil, and placed in a supine position and their abdomens were shaved. After laparotomy was performed, an incision of 1 cm was created on the left abdominal sidewall below the epigastric vessel by using a scalpel to excise the peritoneum. The muscle under serosal surface was disrupted and hemorrhaged, but not perforated. Then, sutured around the periphery of the lesion and a knot was tied in each corner and along each side of the square to stimulate adhesion formation. Rats were assigned in equal numbers to a treated and control group. Rats of the control group were not covered with any anti-adhesion barrier (group I). In the treatment group, the sidewall defect was covered with a piece (2 cm × 2 cm) of calcium alginate (group II) or chitosan alginate (group III) ES mat. Afterwards, the closure of the peritoneal cavity was performed. After 7 days, abdominal walls and the incision line were investigated with regard to formation of adhesions. The adhesions were scaled according to the scoring method developed by Yang et al. (2009).

2.8. Histological analysis

Tissue was collected, treated with formaldehyde (10%), and embedded in paraffin. Then the samples were cut into sections of 4 μm in thickness by cryomicrotome (Leica RM 2145, Nussloch, Germany). After tissue sections were dewaxed and rehydrated conventionally, sections were stained with Masson's Trichrome Staining kit (HT15, Sigma, USA). By this staining, the collagen would be stained as blue, while keratin would be stained as red. The stained samples were then examined using an optical microscope.

3. Results and discussion

3.1. Morphology of ES mats

In this study, ES mats were composing of alginate and chitosan. Fig. 1A shows the photographs and SEM images of chitosan alginate and calcium alginate. Fig. 1B shows that the green alginate fibers were overlapping with the red chitosan fibers for the chitosan alginate ES mat. This suggests that alginate was indeed coagulated by chitosan during electrospinning.

3.2. Disintegration test

Fig. 2 shows the morphological changes of ES mat after soaking in DMEM for 1, 3, and 5 days. After 1 day, calcium alginate and chitosan alginate mats did not change in the morphology (Fig. 2A and D). After 3 days, some of the calcium alginate fibers became flat, suggesting dissolution (Fig. 2B). On the contrary, chitosan alginate exhibited no significant morphological change at the 3rd day (Fig. 2E). After 5 days, the calcium alginate mat became more membrane-like rather than fibrous structure (Fig. 2C). At the same time, chitosan alginate fibers exhibited slight dissolution (Fig. 2F). Fig. 2G summarizes the change in weight of ES mats when soaking in DMEM. After 5 days, approximately 57% and 37% of calcium alginate and chitosan alginate mats lost, respectively. The disintegration of calcium alginate was much faster than chitosan alginate. This can be attributed to the exchange of calcium ion with sodium ion from DMEM, causing the disintegration of calcium alginate (Bajpai & Sharma, 2004).

3.3. Cell culture study

Fig. 3A shows the microscopic observations of L929 cells cultured 48 h on an ECIS chip. Comparing with the control and the

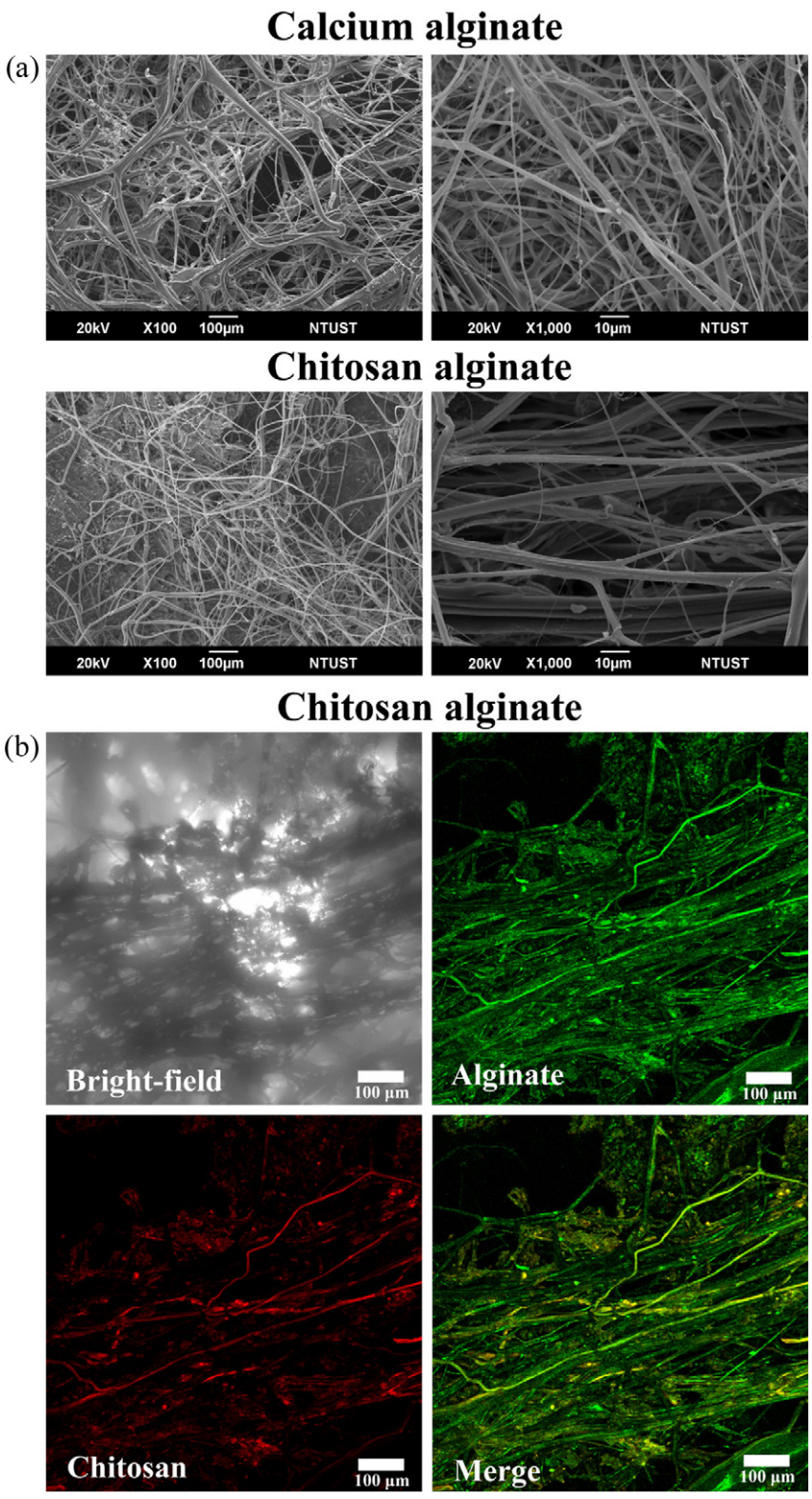

Fig. 1. Representative images of the electrospun mats. (A) SEM micrograph; and (B) CLSM micrographs.

calcium alginate groups, the population of the L929 cells cultured with chitosan alginate was less dense with abnormal morphology. Fig. 3B shows the effect of alginate and chitosan on the growth of L929 cells. The cell growth was not much affected in the presence of alginate. On the other hand, in the presence of chitosan, the cell growth was inhibited in the first 84 h after treatment, and then began to decline. This is again the evidence that chitosan can inhibit the growth of fibroblasts.

Fig. 3C shows that the effect of ES mats on the growth of L929. Only the impedance for the cells cultured with the extract of chitosan alginate decreased with the time. This suggests that the presence of chitosan can inhibit the activity of L929 fibroblast cell.

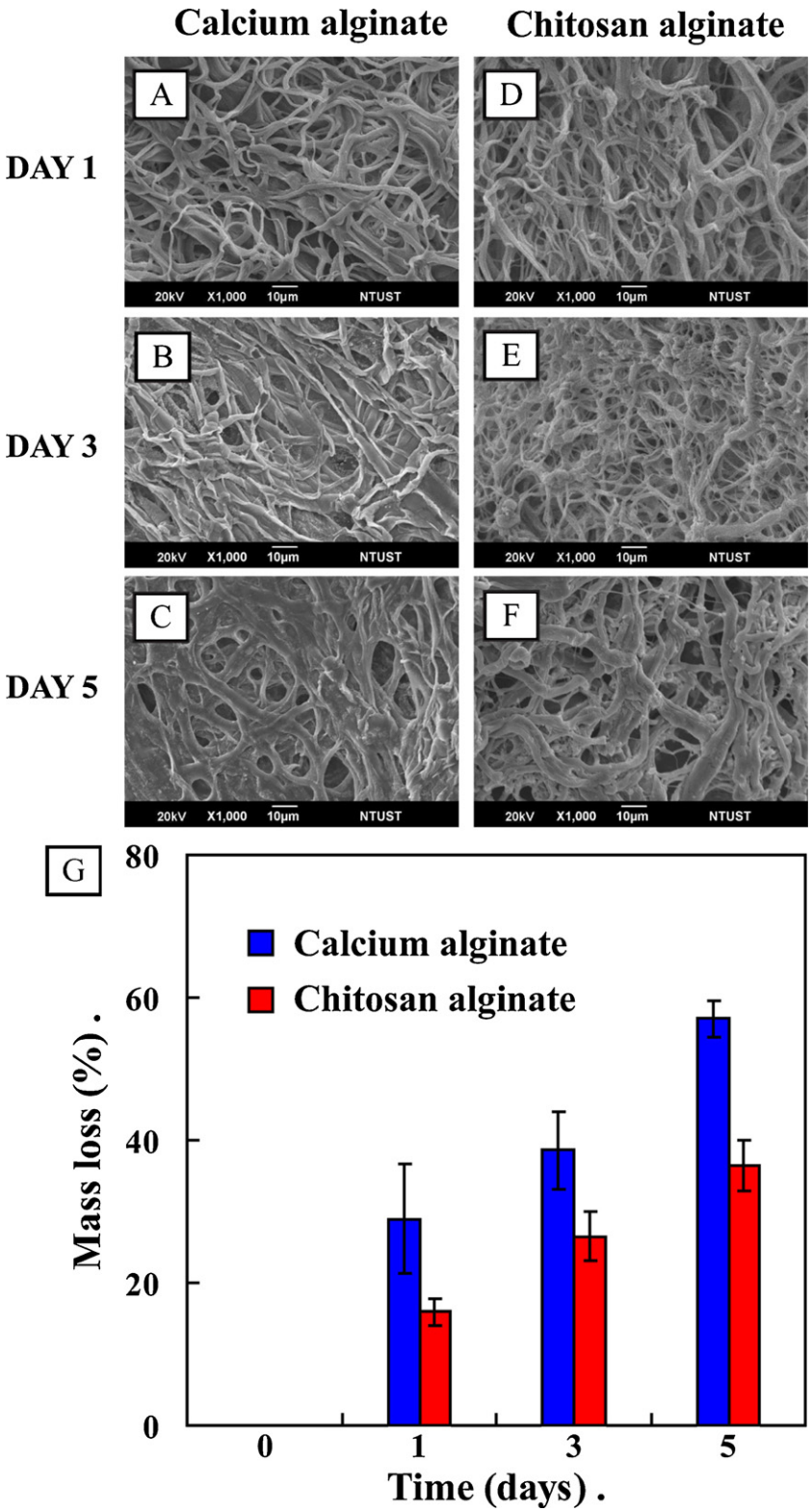

Fig. 2. Disintegration tests. (A)–(C) SEM images of calcium alginate; (D)–(F) SEM images of chitosan alginate, and (G) the mass loss of the electrospun mats in DMEM at 37 °C over time.

All the results in Fig. 3 are in agreement, indicating that chitosan can inhibit the growth of fibroblasts. The mechanism of the inhibition can be studied by the MTT assay and flow cytometry in the following sections.

The evaluation of cytotoxicity is very important for the materials in biomedical applications. MTT assay was used to evaluate the in vitro cytotoxicity of ES mats. MTT assay is a quick effective method for testing mitochondrial impairment and correlates quite well with cell proliferation.

Fibroblasts, which invade the wound in the first few days of healing, have multiple functions important to wound repair, such as collagen synthesis, ECM reorganization, and wound contraction

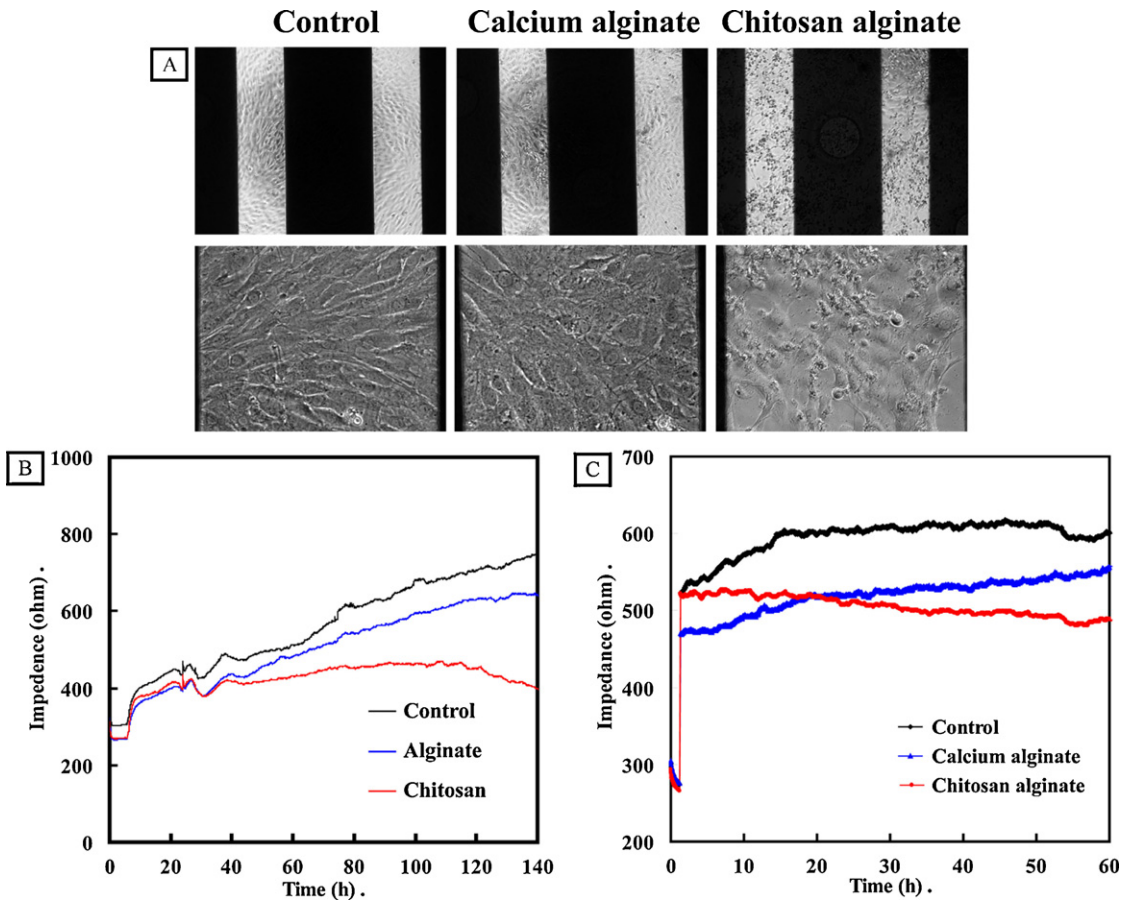

Fig. 3. ECIS measurement. (A) Microscopic observation of the L929 on an ECIS chip. (B) ECIS assay with pure constituents, and (C) with extract of the anti-adhesion barriers.

resulting in mature scar formation. The healing processes of normal peritoneal tissue repair or development of adhesions include migration, proliferation, and/or differentiation of several cell types such as inflammatory cells, mesothelial cells, and fibroblasts (Saed & Diamond, 2002).

Fig. 4 shows the time-course of fibroblasts proliferated on the ES mats. Although L929 cells proliferated on calcium alginate and chitosan alginate, the proliferation rate on chitosan alginate was slower than that on calcium alginate. On the 5th day, the number of cells on chitosan alginate mat was 66% of that on calcium alginate mat. In the literature, fibroblasts could not proliferation on the surface of chitosan film (Chatelet, Damour, & Domard, 2001; Sangsanoh et al., 2010). In addition, fibroblasts cultured on the dibutyryl chitin non-woven materials exhibited non-adhesive behavior (Muzzarelli et al., 2005). Our results agree with their findings. This is favorable for the purpose of anti-adhesion.

Apoptosis is a programmed, physiological mode of cell dearth that plays a key role in tissue homeostasis (Engeland, Nieland, Ramaekers, & Schutte Bert Reutelingsperger, 1998). Apoptosis may be inhibited by deleterious stimuli such as hypoxia, contorting the balance of cellular proliferation, differentiation, and death, hence impairing the normal peritoneal wound repair process (Saed & Diamond, 2002). Recently, it has become clear that biomaterials may activate different pathways leading to apoptosis and necrosis. Exogenous stimuli triggering apoptosis are including hypoxia, radiation, and chemotherapeutic drugs (Saed et al., 2010). In addition, the identification of the mechanism of cell damage/death induced by biomaterials is particularly important in the assessment of the biological reaction to implanted devices (Mao et al., 2004).

Fluorescent probe Annexin V is commonly used for the quantification of apoptosis, because it binds to phosphatidylserine (PS) exposing on the surface of apoptotic cells. PI is a stain frequently used to identify necrotic cells, based upon the loss of membrane

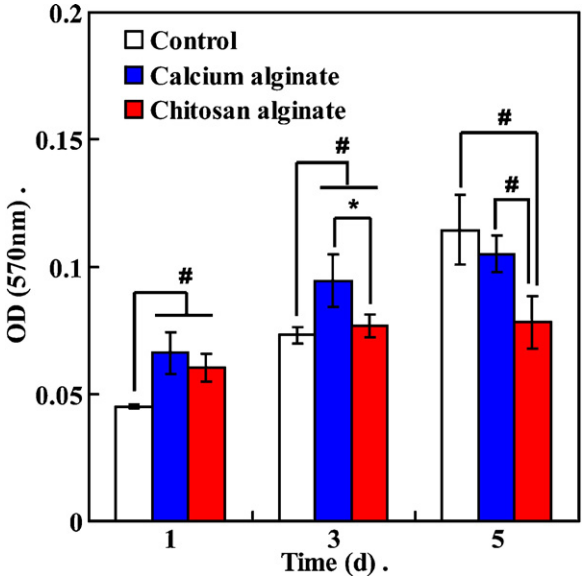

Fig. 4. Proliferation of fibroblast cultured on electrosupn mats (control: TCPS). Data are presented as mean ± standard deviation with $n = 6$ ($^{*}p < 0.05$, $\#p < 0.01$).

integrity (Mao et al., 2004). Apoptotic cells maintain plasma membrane integrity during the major portion of the apoptotic process and become permeable to PI only during secondary necrosis (Faria, Cardoso, Larson, Silva, & Rossi, 2009). Necrosis is usually considered to be from physical injury and is not genetically controlled (Ciapetti et al., 2002). However, early apoptotic cells are Annexin V positive and PI negative, and late apoptotic or already dead cell are positive to both Annexin V and PI.

In order to assess the effect of ES mat on apoptosis, L929 cells were incubated with different ES mats. Fig. 5A–C shows that the contour diagrams of Annexin V and PI stained L929 cells using flow cytometry after 24 h of incubation with different ES mats. Fig. 5B shows that apoptosis was only 1.7% for L929 cell incubating with calcium alginate mat. On the other hand, Fig. 5C shows that early apoptosis ($Annexin^+, PI^-$) was 12.4% when incubating with chitosan alginate. The results suggest that only with the presence of chitosan, apoptosis in L929 would occur in a significant level. Previous study reported that chitosan may interact with the cell membrane to trigger apoptosis (Hasegawa, Yagi, Iwakawa, & Hirai, 2001). Therefore the anti-adhesion can be attributed to the chitosan in the chitosan alginate ES mat.

3.4. *In vivo application and evaluation of peritoneal adhesion prevention efficacy*

In this work, peritoneal adhesion was induced in rats using a cecal abrasion-abdominal sidewall defect model because peritoneum is one of the tissues that adhesion frequently occurs after surgical treatment. The purpose of this animal study was to evaluate the effects of ES mat on the tissue anti-adhesion. All animals remained healthy throughout the experiment.

Fig. 6A shows the photographs of the surgical site when the animals were sacrificed after 1 week postsurgery. Fig. 6A shows that the animals without any treatment of their peritoneal defects exhibited dense adhesions between the injured cecum and abdominal wall and that were difficult to dissect. Fig. 6B shows that the percentage of high-grade adhesion (total of score 2 and score 3) of the untreated group was 90%. The group implanted with calcium alginate mat also showed dense adhesion, and that the percentage of high-grade adhesion was 80%. On the other hand, about 40% of the chitosan alginate group exhibited no tissue adhesion between injured peritoneum and cecum. In addition, no adhesion of score 3 was observed in the chitosan alginate group. This suggested that the chitosan alginate may effectively reduce peritoneal tissue adhesion, hence chitosan alginate mat may be applicable as a tissue adhesion barrier material.

3.5. *Histological analysis*

Fig. 7 shows the histological staining of the adhesion site in rat models. Fig. 7A shows the image of histological section of normal rat peritoneal. Both Fig. 7B and C shows thicker adhesion layer, suggesting the wound treated with calcium alginate was not much different from the wound without treatment. Fig. 7D shows that the adhesion layer was thinner than Fig. 7B and C when treating with chitosan alginate. In addition, fewer blood cells were observable in the adhesion layer, indicating that the treating effect with chitosan alginate was better than calcium alginate.

Masson tritchrome staining was employed to explore the overall distribution and density of regenerated collagen from fibroblast after surgical treatment. Fig. 7E–H shows the histological examination of abdominal wall adhesions with and without treatments. Fig. 7F shows that without treatment, the adhesion layer on the abdominal wall was thicker and was composed mostly of collagen fibers scattering with few muscle fibers. Fig. 7G shows that when treating with calcium alginate, the structure of the adhesion layer was similar to that in Fig. 7F. Fig. 7H shows that when treating with chitosan alginate, the adhesion layer was thinner and was similar to the normal tissue shown in Fig. 7E. This suggests that adhesions were reduced, and the injured site was re-epithelialized.

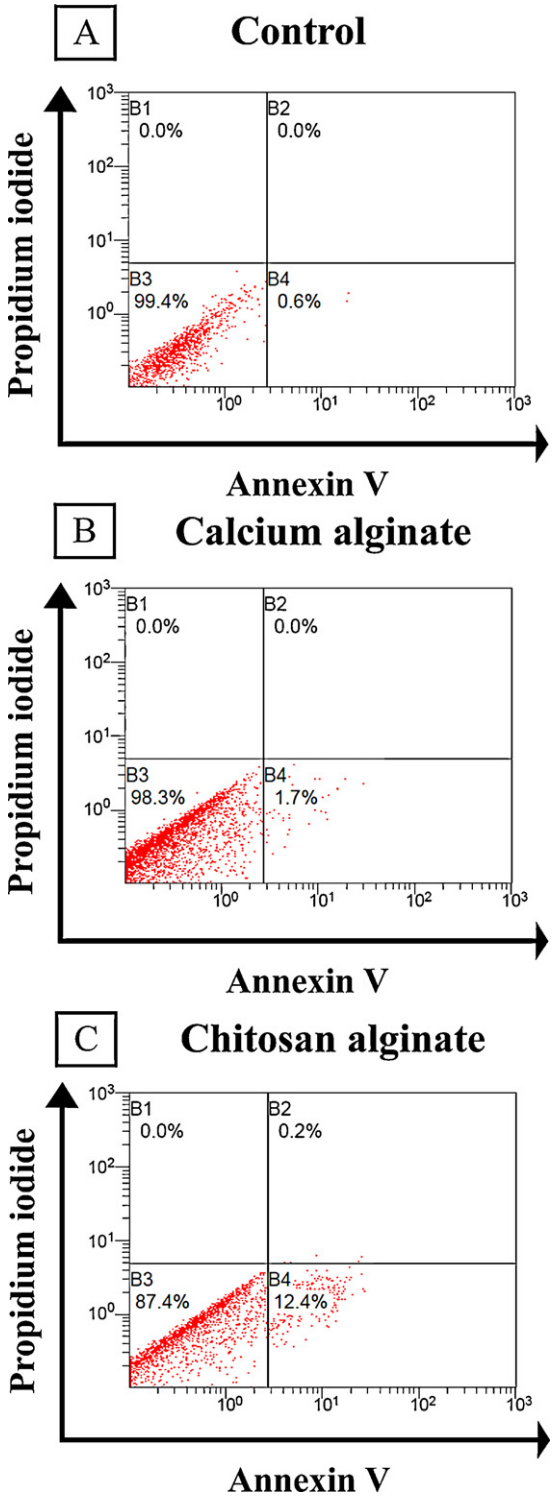

Fig. 5. The flow cytometric analysis of FITC-Annexin V-PI stained L929 fibroblast cell after culturing for 1 day. (A) Control (TCPS); (B) calcium alginate; (C) chitosan alginate.

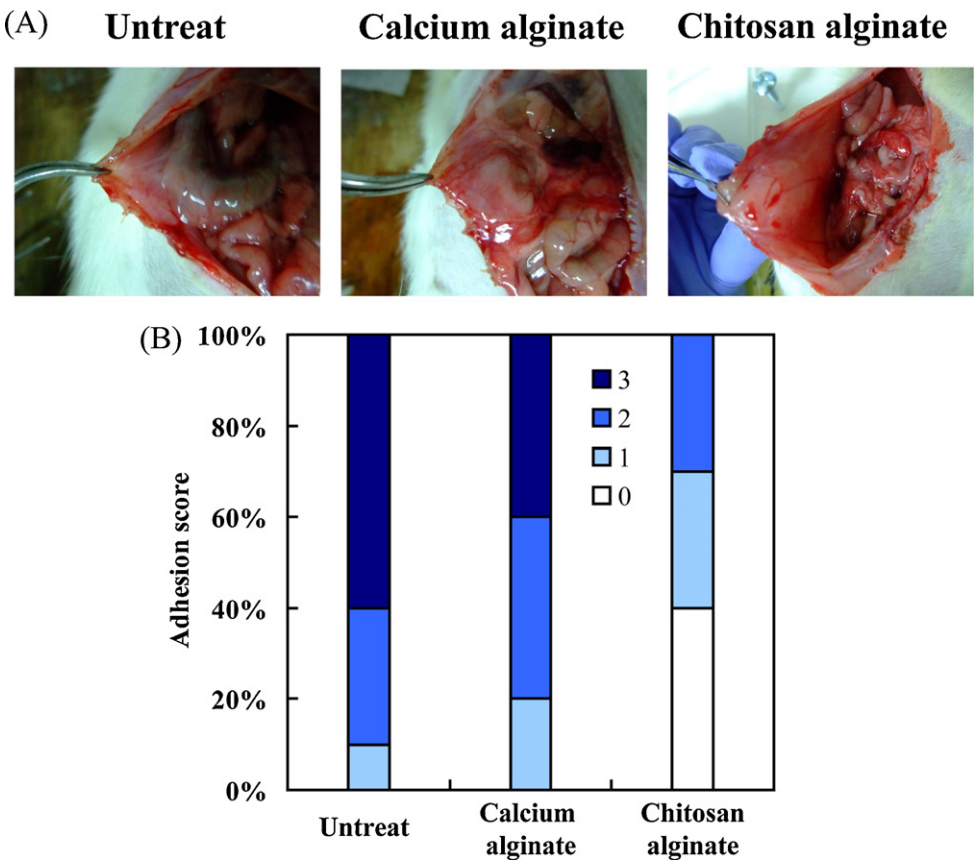

Fig. 6. In vivo tests using Wistar rat model. (A) Peritoneums 1 week after implanting anti-adhesion barriers. (B) Distribution of adhesion scores for calcium alginate and chitosan alginate mats or for untreated peritoneum (score 0: no adhesion; score 1: mild, easily separable intestinal adhesion; score 2: moderate intestinal adhesion, separable by blunt dissection; score 3: severe intestinal adhesion, adhesion requiring sharp dissection).

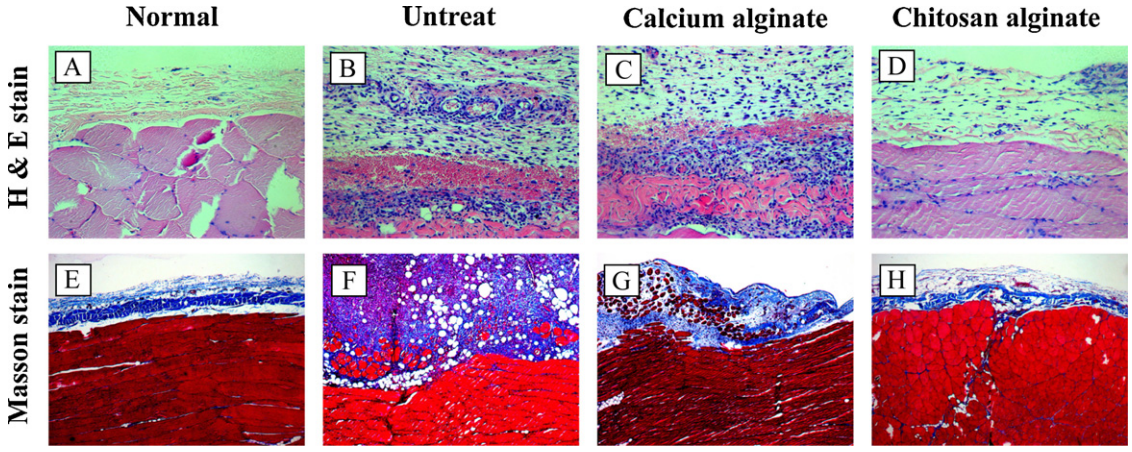

Fig. 7. Histological staining of the adhesion site. (A)–(D) Sections stained with hematoxylin–eosin (40×); and (E)–(H) Masson's trichrome stain.

4. Conclusions

In this paper, we have successfully prepared a novel tissue anti-adhesion barrier based on electrospinning mat for reducing peritoneal adhesion. Unlike earlier electrospun barriers, such a barrier is composing of two carbohydrates: alginate and chitosan. Both alginate and chitosan are biodegradable when implanted. They also exhibit favorable interaction with the adjacent tissues to inhibit tissue adhesion: alginate can reduce cell adhesion and protein adsorption and chitosan can inhibit proliferation and trigger apoptosis. In addition, such electrospinning mat is water swellable, making it flexible and causing less stimulus–response. Therefore, both macroscopic and histological observations showed that chitosan alginate mat was highly effective in reducing the formation of postoperative abdominal adhesions in vivo. These results indicated that chitosan alginate could be a tissue anti-adhesion barrier owing to its efficient tissue anti-adhesion performance.

Acknowledgements

The authors would like to thank the National Science Council of Taiwan, Republic of China, for financially supporting this research

under Grants NSC-100-2120-M-038-022, and NSC-98-2320-B-002-043-MY3. The authors would also like to thank National Taiwan University Hospital for providing Grant NTUH 100-S1661.

References

Agarwal, S., Wendorff, J. H., & Greiner, A. (2008). Use of electrospinning technique for biomedical applications. *Polymer*, *49*, 5603–5621.

Agarwal, S., Wendorff, J. H., & Greiner, A. (2009). Progress in the field of electrospinning for tissue engineering applications. *Advanced Materials*, *21*, 3343–3351.

Anraku, M., Fujii, T., Kondo, Y., Kojima, E., Hata, T., Tabuchi, N., et al. (2011). Antioxidant properties of high molecular weight dietary chitosan in vitro and in vivo. *Carbohydrate Polymers*, *83*, 501–505.

Bajpai, S. K., & Sharma, S. (2004). Investigation of swelling/degradation behaviour of alginate beads crosslinked with Ca^{2+} and Ba^{2+} ions. *Reactive and Functional Polymers*, *59*, 129–140.

Bhattarai, N., Gunn, J., & Zhang, M. (2010). Chitosan-based hydrogels for controlled, localized drug delivery. *Advanced Drug Delivery Review*, *62*, 83–99.

Bölgen, N., Vargel, İ., Korkusuz, P., Menceloğlu, Y. Z., & Pişkin, E. (2007). In vivo performance of antibiotic embedded electrospun PCL membranes for prevention of abdominal adhesions. *Journal of Biomedical Materials Research Part B – Applied Biomaterials*, *81B*, 530–543.

Cashman, J. D., Kennah, E., Shuto, A., Winternitz, C., & Springate, C. M. K. (2010). Fucoidan film safely inhibits surgical adhesions in a rat model. *Journal of Surgical Research*, *171*, 495–503.

Chang, J. J., Lee, Y. H., Wu, M. H., Yang, M. C., & Chien, C. T. (2012). Preparation of electrospun alginate fibers with chitosan sheath. *Carbohydrate Polymers*, *87*, 2357–2361.

Chatelet, C., Damour, O., & Domard, A. (2001). Influence of the degree of acetylation on some biological properties of chitosan films. *Biomaterials*, *22*, 261–268.

Chuang, Y. C., Fan, C. N., Cho, F. N., Kan, Y. Y., Chang, Y. H., & Kang, H. Y. (2008). A novel technique to apply a seprafilm (hyaluronate-carboxymethylcellulose) barrier following laparoscopic surgeries. *Fertility and Sterility*, *90*, 1959–1963.

Ciapetti, G., Granchi, D., Savarino, L., Cenni, E., Magrini, E., Baldini, N., et al. (2002). In vitro testing of the potential for orthopedic bone cements to cause apoptosis of osteoblast-like cells. *Biomaterials*, *23*, 617–627.

Diamond, M. P., Luciano, A., Johns, D. A., Dunn, R., Young, P., & Bieber, E. (2003). Reduction of postoperative adhesions by N,O-carboxymethylchitosan: A pilot study. *Fertility and Sterility*, *80*, 631–636.

Engeland, M., Nieland, L. J. W., Ramaekers, F. C. S., & Schutte Bert Reutelingsperger, C. P. M. (1998). Annexin V-affinity assay: A review on an apoptosis detection system based on phosphatidylserine exposure. *Cytometry*, *31*, 1–9.

Faria, G., Cardoso, C. R. B., Larson, R. E., Silva, J. S., & Rossi, M. A. (2009). Chlorhexidine-induced apoptosis or necrosis in L929 fibroblasts: A role for endoplasmic reticulum stress. *Toxicology and Applied Pharmacology*, *234*, 256–265.

George, M., & Abraham, T. E. (2006). Polyionic hydrocolloids for the intestinal delivery of protein drugs. Alginate and chitosan – A review. *Journal of Controlled Release*, *114*, 1–14.

Giaever, I., & Keese, C. R. (1984). Monitoring fibroblast behavior in tissue culture with an applied electric field. *Proceedings of the National Academy of Sciences of the United States of America*, *81*, 3761–3764.

Hasegawa, M., Yagi, K., Iwakawa, S., & Hirai, M. (2001). Chitosan induces apoptosis via caspase-3 activation in bladder tumor cells. *Cancer Science*, *92*, 459–466.

Jeong, S. I., Krebs, M. D., Bonino, C. A., Khan, S. A., & Alsberg, E. (2010). Electrospun alginate nanofibers with controlled cell adhesion for tissue engineering. *Macromolecular Bioscience*, *10*, 934–943.

Kayaoglu, H. A., Ozkan, N., Hazinedaroglu, S. M., Ersoy, O. F., & Koseoglu, R. D. (2005). An assessment of the effects of two types of bioresorbable barriers to prevent postoperative intra-abdominal adhesions in rats. *Surgery Today*, *35*, 946–950.

Lauder, C. I. W., Garcea, G., Strickland, A., & Maddern, G. J. (2011). Use of a modified chitosan–dextran gel to prevent peritoneal adhesions in a rat model. *Journal of Surgical Research*, *171*, 877–882.

Lee, K. Y., Jeong, L., Kang, Y. O., Lee, S. J., & Park, W. H. (2009). Electrospinning of polysaccharides for regenerative medicine. *Advanced Drug Delivery Reviews*, *61*, 1020–1032.

Lee, Y. H., Chang, J. J., Lai, W. F., Yang, M. C., & Chien, C. T. (2011). Layered hydrogel of poly(γ-glutamic acid), sodium alginate, and chitosan: Fluorescence observation of structure and cytocompatibility. *Colloids and Surfaces B: Biointerfaces*, *86*, 409–413.

Lee, S. H., Ryu, B., Je, J. Y., & Kim, S. K. (2011). Diethylaminoethyl chitosan induces apoptosis in HeLa cells via activation of caspase-3 and p53 expression. *Carbohydrate Polymers*, *84*, 571–578.

Li, Z., Ramay, H. R., Hauch, K. D., Xiao, D., & Zhang, M. (2005). Chitosan–alginate hybrid scaffolds for bone tissue engineering. *Biomaterials*, *26*, 3919–3928.

Mao, J. S., Cui, Y. L., Wang, X. H., Sun, Y., Yin, Y. J., Zhao, H. M., et al. (2004). A preliminary study on chitosan and gelatin polyelectrolyte complex cytocompatibility by cell cycle and apoptosis analysis. *Biomaterials*, *25*, 3973–3981.

McCoy, M. H., & Wang, E. (2005). Use of electric cell–substrate impedance sensing as a tool for quantifying cytopathic effect in influenza A virus infected MDCK cells in real-time. *Journal of Virological Methods*, *130*, 157–161.

Muzzarelli, R. A. A. (2009). Chitins and chitosans for the repair of wounded skin, nerve, cartilage and bone. *Carbohydrate Polymers*, *76*, 167–182.

Muzzarelli, R. A. A. (2010). Chitins and chitosans as immunoadjuvants and non-allergenic drug carriers. *Marine Drugs*, *8*, 292–312.

Muzzarelli, R. A. A. (2011). Biomedical exploitation of chitin and chitosan via mechano-chemical disassembly, electrospinning, dissolution in imidazolium ionic liquids, and supercritical drying. *Marine Drugs*, *9*, 1510–1533.

Muzzarelli, R. A. A., Guerrieri, M., Goteri, G., Muzzarelli, C., Armeni, T., Ghiselli, R., et al. (2005). The biocompatibility of dibutyryl chitin in the context of wound dressings. *Biomaterials*, *26*, 5844–5854.

Paulo, N. M., de Brito e Silva, M. S., Moraes, Â. M., Rodrigues, A. P., de Menezes, L. B., Miguel, M. P., et al. (2009). Use of chitosan membrane associated with polypropylene mesh to prevent peritoneal adhesion in rats. *Journal of Biomedical Materials Research Part B: Applied Biomaterials*, *91B*, 221–227.

Pillai, C. K. S., Paul, W., & Sharma, C. P. (2009). Chitin and chitosan polymers: Chemistry, solubility and fiber formation. *Progress in Polymer Science*, *34*, 641–678.

Rutledge, G. C., & Fridrikh, S. V. (2007). Formation of fibers by electrospinning. *Advanced Drug Delivery Reviews*, *59*, 1384–1391.

Saed, G. M., & Diamond, M. P. (2002). Apoptosis and proliferation of human peritoneal fibroblasts in response to hypoxia. *Fertility and Sterility*, *78*, 137–143.

Saed, G. M., Jiang, Z. L., Fletcher, N. M., Arab, A. A., Diamond, M. P., & Abu-Soud, H. M. (2010). Exposure to polychlorinated biphenyls enhances lipid peroxidation in human normal peritoneal and adhesion fibroblasts: A potential role for myeloperoxidase. *Free Radical Biology & Medicine*, *48*, 845–850.

Sangsanoh, P., Suwantong, O., Neamnark, A., Cheepsunthorn, P., Pavasant, P., & Supaphol, P. (2010). In vitro biocompatibility of electrospun and solvent-cast chitosan substrata towards Schwann, osteoblast, keratinocyte and fibroblast cells. *European Polymer Journal*, *46*, 428–440.

Tomida, Yasufuku, H., Fujii, T., Kondo, T., Kai, Y., & Anraku, T. (2010). M Polysaccharides as potential antioxidative compounds for extended-release matrix tablets. *Carbohydrate Research*, *345*, 82–86.

Ward, B. C., & Panitch, A. (2011). Abdominal adhesions: Current and novel therapies. *Journal of Surgical Research*, *165*, 91–111.

Way, T. D., Hsieh, S. R., Chang, C. J., Hung, T. W., & Chiu, C. H. (2010). Preparation and characterization of branched polymers as postoperative anti-adhesion barriers. *Applied Surface Science*, *256*, 3330–3336.

Yang, D. J., Chen, F., Xiong, Z. C., Xiong, C. D., & Wang, Y. Z. (2009). Tissue anti-adhesion potential of biodegradable PELA electrospun membranes. *Acta Biomaterialia*, *5*, 2467–2474.

Yeo, Y., & Kohane, D. S. (2008). Polymers in the prevention of peritoneal adhesions. *European Journal of Pharmaceutics and Biopharmaceutics*, *68*, 57–66.

Yeo, Y., Burdick, J. A., Highley, C. B., Marini, R., Langer, R., & Kohane, D. S. (2006). Peritoneal application of chitosan and UV-cross-linkable chitosan. *Journal of Biomedical Materials Research*, *78A*, 668–675.

Zhang, Z. L., Xu, S. W., & Zhou, X. L. (2006). Preventive effects of chitosan on peritoneal adhesion in rats. *World Journal of Gastroenterology*, *12*, 4572–4577.

Zong, X., Li, S., Chen, E., Garlick, B., Kim, K. S., Fang, D., et al. (2004). Prevention of postsurgery-induced abdominal adhesions by electrospun bioabsorbable nanofibrous poly(lactide-co-glycolide)-based membranes. *Annals of Surgery*, *240*, 910–915.